Impact toughening of polycarbonate by microcellular foaming

Dimitris I. Collias* and Donald G. Baird
Chemical Engineering Department, Virginia Polytechnic Institute and State University, Blacksburg, VA 24061, USA

and Rein J. M. Borggreve
DSM Research, 6160 Geleen, The Netherlands
(Received 29 November 1993; revised 25 January 1994)

The microcellular foams of polycarbonate (PC) were studied to gain an understanding of the effect that small bubbles have on the impact properties. The PC matrix was selected based on its intrinsic ductility. Sharply and bluntly notched samples were tested in Charpy impact configuration, so that the effects of the sharpness of the notch could also be studied. Sharply notched microcellular PC exhibited the most promising behaviour. The maximum load of foamed PC was substantially improved over that of unfoamed PC. Furthermore, the impact toughness (total energy absorbed) per unit thickness improved dramatically over that of the unfoamed PC. This effect is explained by the fact that the presence of small bubbles induces a transition from brittle to ductile behaviour by relieving the triaxial stress condition in front of the crack tip.

(Keywords: polycarbonate; microcellular foams; impact toughness)

INTRODUCTION

The use of substantial volume fraction of extremely small rubber particles blended in polymer matrices is a well known technique for the improvement of the impact toughness of both crazing and shearing matrices. The function of these rubber particles in shearing matrices is to relieve the triaxial stress state (plane-strain conditions) at the crack tip by internal cavitation and to allow shear yielding to occur[1].

The question of whether the polymer matrix deforms by crazing or shear yielding depends on both extrinsic parameters, such as the stress state (loading mode, sample dimensions, notch geometry and tensile speed) and temperature, as well as intrinsic parameters, such as the molecular structure and microstructure or morphology. In rubber-modified glassy polymers, it was shown by van der Sanden *et al.*[2,3] that the deformation mode depends on the distance between the rubber particles (also called interparticle surface-to-surface distance, ID, or ligament thickness). Below a critical ligament thickness, ID_c, the deformation mode is shearing, whereas above ID_c it is crazing. The critical ligament thickness is a function of the yield stress of the polymer, its entanglement density[3] and the orientation direction[4]. For example, polystyrene (PS) has a very small critical ligament thickness of about 0.05 μm when unoriented[3], since it has a low entanglement density or, equivalently, a large entanglement molecular weight.

Polycarbonate (PC), on the other hand, has a low entanglement molecular weight and its critical ligament thickness is relatively large[3]. PC is ductile under tensile testing at moderate speed, even when it is unmodified. The ductility of PC is related not only to its high entanglement density, but also to the mobility of its polymer chains. This can be deduced from the position of the broad G'' maximum in the low-temperature range (so-called γ-relaxation)[5] at -105°C. When the PC chain is modified with substituents (e.g. methyl groups, as in tetramethylbisphenol-A polycarbonate) the γ-relaxation is broadened and shifted to 50°C, and simultaneously the intrinsic ductility decreases[5]. The relation between the polymer chain mobility and the intrinsic toughness is not completely understood, but it is suggested that stored elastic energy in the material can be transformed into plastic deformation more easily when polymer chains have better possibilities to undergo conformational changes[6]. However, under impact conditions, especially in the presence of a sharp notch, PC is brittle. The brittle-to-ductile transition depends strongly on extrinsic parameters, such as sample thickness, notch tip radius, loading rate, temperature, etc., as modelled by Brown[7]. On the other hand, during fracture of specimens with blunt notches, both crazing and shear yielding may be present simultaneously[8].

Since the toughening mechanisms start with rubber-particle cavitation in order to relieve the triaxial stress state, the question has been raised many times of whether microbubbles could be substituted for the rubber particles. In particular, the question of whether or not microbubbles can be effective in toughening PC under

* To whom correspondence should be addressed. Present address: The Procter & Gamble Co., Winton Hill Technical Center, 6110 Center Hill Road, Cincinnati, OH 45224, USA

0032-3861/94/18/3978–06

impact conditions is still a subject of much speculation, as Sue *et al.* recently pointed out[9].

This idea of using microbubbles in order to toughen plastics was first implemented by Martini *et al.*[10] and the resulting structure was called microcellular foam (MCF). MCFs have an average bubble diameter on the order of 10 μm, and density reduction (or bubble volume fraction) of about 20–40%. Microcellular foaming, besides being useful in exploring the toughening of polymer matrices, is also useful in foaming plastic parts of very small dimensions, where only microbubbles are allowed to grow. As far as the impact properties of MCFs are concerned, only one set of impact experiments has been reported. Waldman[11] measured the notched Charpy impact toughness of MCFs of PS and found it to be higher than that of the neat polymer, whereas in a falling weight experiment the impact toughness was reported to be less than that of the neat polymer matrix.

At present, MCFs can be produced by four techniques, namely phase separation, gas supersaturation, precipitation with a compressed fluid antisolvent, and polymerization of monomers (however, there may be more practical ways). In this paper we will consider only the second technique. For glassy polymers, it consists of the following steps: initially, saturating the polymer matrix with gas under high pressure; creating supersaturation (or oversaturation) conditions by releasing the gas pressure; finally, foaming the polymer matrix by heating it above the glass transition temperature.

This paper reports on the impact behaviour of MCFs of PC, and is part of a series of papers on the tensile and impact behaviour of MCFs of PC, PS and styrene–acrylonitrile copolymer[12,13].

EXPERIMENTAL

The polymer matrix was polycarbonate Lexan® 141 from GE. No nucleation sites, were used. The specimens were small rectangular polymer bars cut from the middle part of larger dogbone-shaped injection-moulded bars. The length, L, of the rectangular bars was 63.53 mm, the depth, D, or width, W, was 12.71 mm and the thickness, B, was 3.18 mm. The geometry of these bars is shown in *Figure 1*.

These PC polymer bars were foamed by a procedure similar to that followed by Collias and Baird[12,13], namely the gas supersaturation technique. First, the polymer bars were saturated with nitrogen as in a pressure vessel (autoclave) at 6.34 MPa (920 psi) pressure and at 110°C, for 19 h. The concentration of nitrogen gas at the centre of the bar was estimatged to be 90% of that at the surface at the end of the saturation step. The nitrogen gas was selected as the foaming gas based on its inertness and good properties for microcellular foaming, i.e. low diffusivity and solubility[12]. In the second step, the bars were supersaturated by releasing the nitrogen pressure, and preparation for foaming was carried out by tying the bars to shallow U-channels so that they did not warp during heating in the next step. Finally, in the third step, the bars were foamed by placing them inside an oil bath, kept at a foaming temperature of 165°C, for a period of time, called foaming time. This foaming temperature was slightly higher than the glass transition temperature of PC (which is about 155°C), so that the hydrodynamic resistance to growth was large and therefore the resulting bubbles were small in diameter[12]. The foaming time

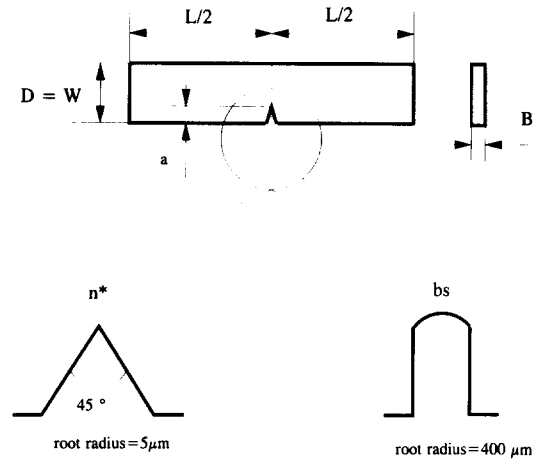

Figure 1 Geometry of bars for the Charpy impact tests. L = span; $D = W$ = depth or width; B = thickness; a = notch length; n^*, sharp notch; *bs*, band saw notch

depends on the desired final bubble diameter and volume fraction. In a second series of experiments, the foaming temperature was increased to 175°C. In all experiments, the samples were quenched after foaming in water at room temperature to inhibit any further growth of the bubbles. The type of foam produced in this way was a closed-cell foam with low bubble volume fraction (less than 30%).

The foamed samples were then notched using two types of notching. The first type of notching included a very sharp notch (referred to as n^*) with a root radius of 5 μm, opening angle of 45° and length of 2.54 mm. This type of notch was made by a sharp notcher (cutting tool; DoAll high-speed steel cutter D-745; DoAll Inc., Madison Heights, MI) turning at a high rotational speed. The effect of notch length on the properties of foamed samples was studied by varying it from 1.27 mm to 5.08 mm. The second type of notching included a rather blunt (wide) notch (referred to as *bs*) with a root radius of 400 μm, parallel edges and 2.54 mm length (see also *Figure 1*). This type of notch was produced by a typical band saw.

Three types of samples were tested, classified on the basis of their thermal and pressure history. The first type included samples foamed as described previously. The second type included samples termed 'blank' samples. These samples underwent the same thermal history as foamed samples, but not the same pressure history[12,13]. In other words, these samples were put into the pressure vessel and stayed there for 19 h at 110°C, without being pressurized with nitrogen gas. Then, they were placed into the oil bath for a period of time, corresponding to the foaming time. These blank samples were then quenched in water at room temperature, notched and tested. In this way, any effect of the thermal history on the results of the foamed samples could be taken into consideration. The third type included samples termed 'supersaturated' samples[12,13]. These samples experienced the same saturation and supersaturation steps as the foamed samples, but they were not subjected to the foaming step. In this way, any effect of pressurized nitrogen in the samples could be taken into consideration. Finally, some of the foamed samples were tested 10 days after foaming, so that any effect of residual nitrogen after foaming could also be studied.

The Charpy tests were carried out using typical Charpy instrumentation at room temperature (25°C). The effects of notch length (1.27, 2.54 and 5.08 mm), notch type (n^* and *bs*) and impact speed (1.0 and 2.5 m s^{-1}) were also analysed to some extent. There were three deviations from the relevant ASTM standards D 256-88. First, the direction of flow during injection moulding was along the length of the bars, while the ASTM standards recommend that the direction of the compression moulding is along the width of the samples. Second, the length of the sample was half that suggested by the standards, and the span between the specimen supports, S, was 40 mm while the standards suggest 95.3 mm. Third, the speed of the pendulum striking the samples at the moment of impact was 1 m s^{-1} whereas the ASTM standards suggest the speed to be 3.46 m s^{-1}.

Finally, the bubble size and number density were studied from scanning electron microscope (SEM) micrographs, which were obtained from a Cambridge Stereoscan 200 microscope (Cambridge Instruments, Cambridge, MA).

RESULTS AND DISCUSSION

The results of the tests are presented in terms of maximum load and total energy (absorbed energy or, equivalently, fracture energy) per unit thickness, and represent the averages of four or five measurements. The total energy corresponds to the total area under the stress–strain curve. The standard deviation for the tests ranged from about 5 to 10% of the mean value.

Unfoamed (neat, untreated, or plain) n^*-notched samples required a total energy per unit thickness of 0.18 J cm^{-1}, whereas for *bs*-notched samples the corresponding figure was 6.72 J cm^{-1}. Supersaturation was shown not to affect the impact tests of unfoamed samples, similarly to the results for tensile tests[12].

Figure 2 shows the effect of foaming on the maximum load of n^*-notched samples. The maximum load of samples foamed at 165°C for 420 s was about 2.5 times that of the neat samples. For shorter foaming times, this increase was steep, whereas for longer times, the increase started decaying at a slow pace. The effect of the foaming temperature on maximum load and foaming time is also shown in *Figure 2*. Increase of the foaming temperature from 165 to 175°C caused a shifting of the maximum load curve towards shorter foaming times and slightly higher levels (about 1.9 times that of the neat samples). The higher foaming temperature is expected to primarily decrease the hydrodynamic resistance of the polymer matrix to bubble growth and to secondarily increase the diffusivity of the foaming gas towards the growing bubbles. As a result, bubble growth was accelerated.

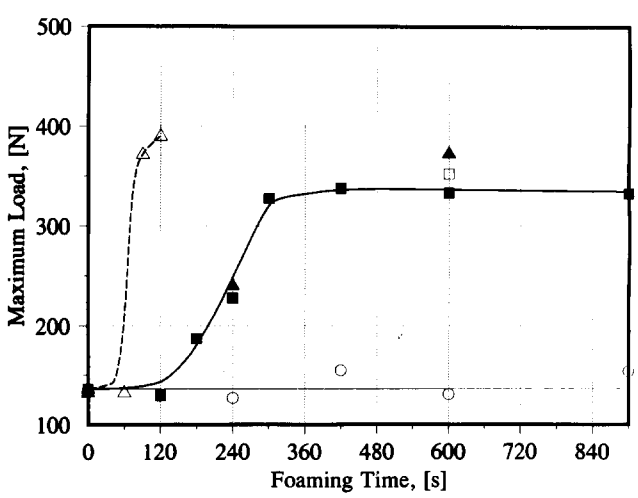

Figure 2 Maximum load of foamed samples with n^*-notch geometry as a function of foaming time. Testing temperature 25°C; impact speed 1.0 m s^{-1}. Foaming temperature: ■, 165°C; △, 175°C. ○, Blank sample; □, foamed sample tested 10 days after foaming; ▲, sample tested at 2.5 m s^{-1} impact speed

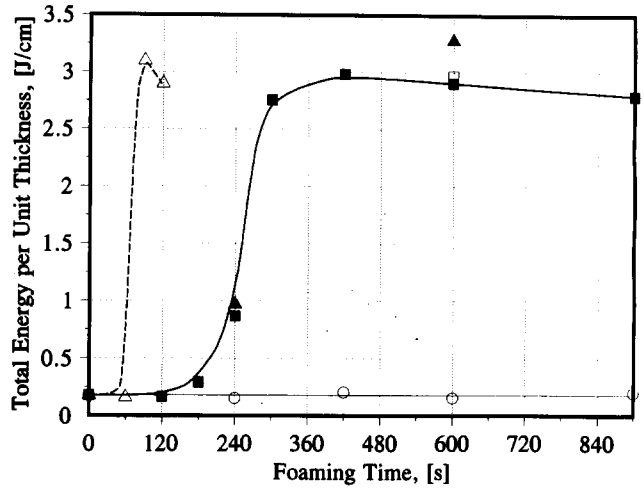

Figure 3 Total energy per unit thickness of foamed samples with n^*-notch geometry as a function of foaming time. Testing temperature 25°C; impact speed 1.0 m s^{-1}. Foaming temperature: ■, 165°C; △, 175°C. ○, Blank sample; □, foamed sample tested 10 days after foaming; ▲, sample tested at 2.5 m s^{-1} impact speed

The maximum load of blank samples, as shown in *Figure 2*, was the same as that of plain samples, and therefore the thermal history had no effect on the maximum load of foamed samples. Furthermore, the maximum load of foamed samples tested 10 days after foaming was the same (to within experimental error) as that of foamed samples tested immediately after foaming. Therefore, consistently with the results from the supersaturated samples, nitrogen gas did not affect the maximum load of microcellular foams of PC. Finally, an increase of the impact speed to 2.5 m s^{-1} caused a slight increase (10–15%) of the maximum load of foamed samples.

Figure 3 shows the dramatic increase of the total energy per unit thickness achieved by microcellular foaming of n^*-notched PC samples. At a foaming time of 420 s, the total energy per unit thickness reached a value about 15.7 times higher than that of the neat PC. For shorter foaming times, this increase was abrupt (S-shaped curve), whereas for longer foaming times the increase decayed very slowly. A 10°C increase of the foaming temperature (i.e. from 165 to 175°C) shifted the total energy curve to shorter times without altering the shape of the curve. This shift was expected, since at higher foaming temperatures the bubble growth process is accelerated. Also, at 175°C foaming temperature, the increase of the total energy per unit thickness relative to that of the unfoamed samples peaked at about 90–120 s, and the corresponding value is 17.3.

Similarly to maximum load, the total energy of blank samples was the same as that of plain samples, and therefore the thermal history did not affect the

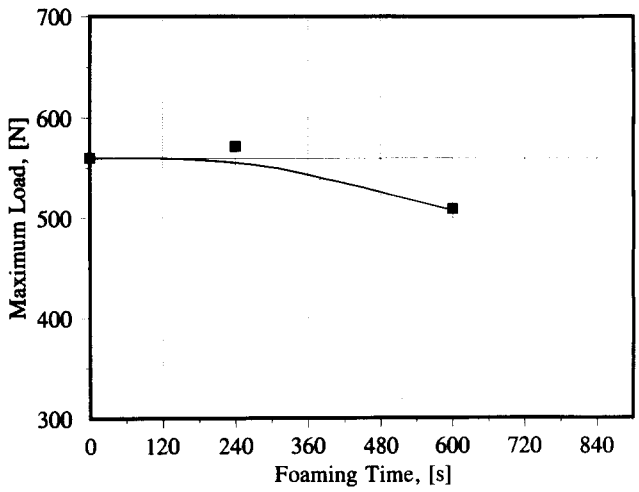

Figure 4 Maximum load of foamed samples with *bs*-notch geometry as a function of foaming time. Foaming temperature 165°C; testing temperature 25°C; impact speed 1.0 m s^{-1}

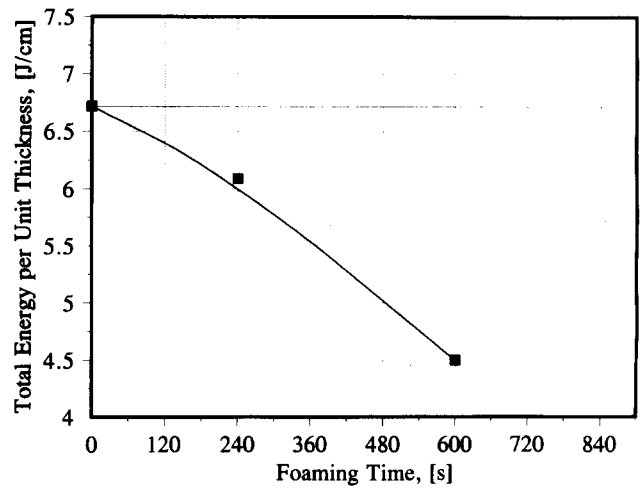

Figure 5 Total energy per unit thickness of foamed samples with *bs*-notch geometry as a function of foaming time. Foaming temperature 165°C; testing temperature 25°C; impact speed 1.0 m s^{-1}

improvements in toughening achieved by microcellular foaming of PC. Furthermore, the total energy of foamed samples tested 10 days after foaming was the same (to within experimental error) as that of foamed samples tested immediately after foaming. Therefore, consistently with the results from the supersaturated samples, nitrogen gas did not affect the total energy of microcellular foams of PC. Finally, an increase of the impact speed caused a slight increase (about 10–15%) of the total energy of foamed samples.

The dramatic behaviour of PC samples with *n**-notch geometry was not duplicated in foamed samples with *bs*-notch geometry. On the contrary, foaming of samples with *bs*-notch geometry decreased slightly the maximum load and the total energy per unit thickness (see *Figures 4* and *5*). Plain PC samples with *bs*-notch geometry already failed in a ductile manner. Upon foaming, the fracture behaviour stayed ductile. However, the amount of absorbed energy decreased, probably as a result of the decreased stiffness of the material.

Figure 6 shows typical load and energy *versus* deflection diagrams for unfoamed and foamed PC samples with *n**-notch geometry. Unfoamed samples exhibit typical brittle behaviour, whereas foamed samples exhibit ductile behaviour. The ductility index of the foamed samples, defined as the ratio of the energy after the maximum load and the total energy, is shown in *Figure 7*, and its shape resembles that of the total energy per unit thickness of *Figure 3*. Note that the ductility of the fracture could also be noticed by the existence of shear lips in the fracture surface.

Both maximum load and total energy per unit thickness are sensitive to the notch length. The smaller the notch length, the higher are the properties, as shown in *Figure 8* for foamed samples with *n**-notch geometry. The average bubble diameter as a function of the foaming time is shown in *Figure 9*. It is interesting to note that the bubble size that gives the best properties, under the conditions of the experiments, is about 40–45 μm in diameter. Thus, the average radius of the bubbles is bigger than the notch tip radius in the *n**-notched samples. One could argue that the effective notch tip radius has been increased, which is the reason for the increase of the impact toughness. However, *Figure 6*

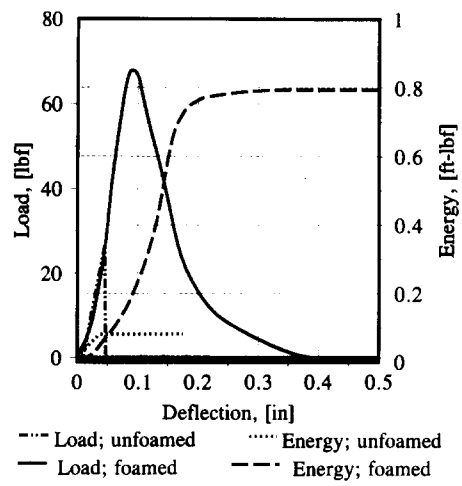

Figure 6 Typical traces for load and total energy *versus* deflection for foamed and unfoamed samples with *n**-notch geometry tested in the Charpy configuration. Testing temperature 25°C; impact speed 1.0 m s^{-1}

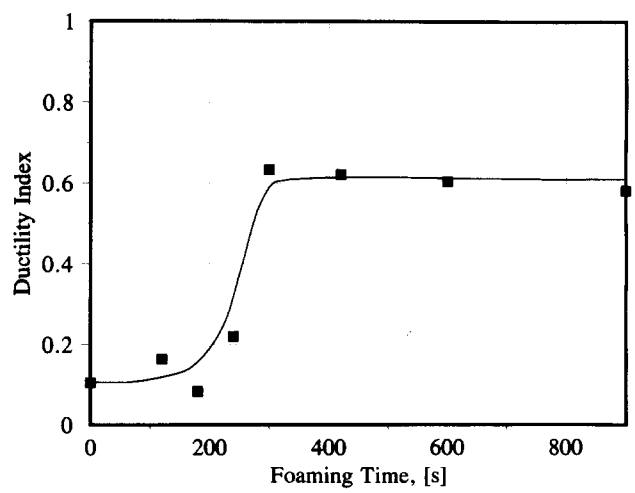

Figure 7 Ductility index as a function of foaming time for samples with *n**-notch geometry foamed at 165°C. Testing temperature 25°C; impact speed 1.0 m s^{-1}

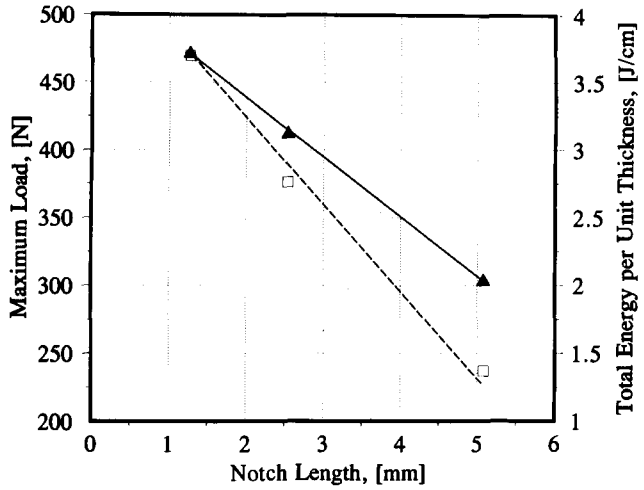

Figure 8 Effect of the notch length on the maximum load and total energy per unit thickness for samples with n^*-notch geometry, foamed for 600 s at 165°C. □, Maximum load; ▲, total energy per unit thickness. Testing temperature 25°C; impact speed 1.0 m s^{-1}

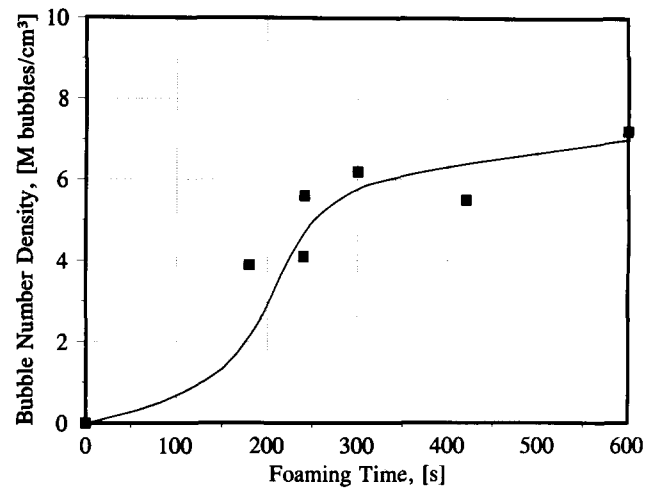

Figure 10 Bubble number density as a function of foaming time for samples with n^*-notch geometry foamed at 165°C

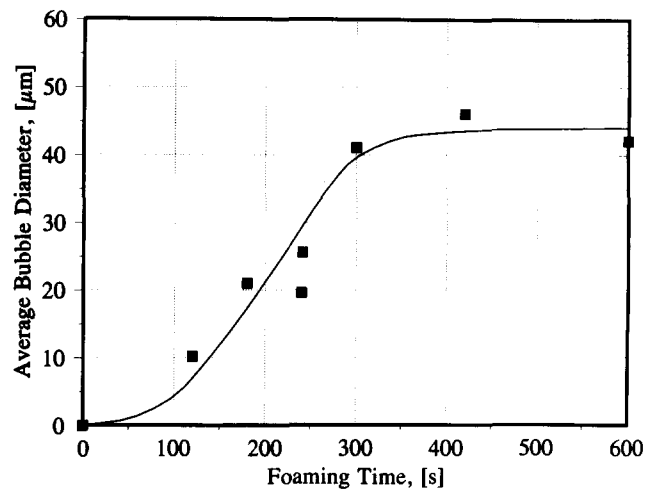

Figure 9 Average bubble diameter as a function of foaming time for samples with n^*-notch geometry foamed at 165°C

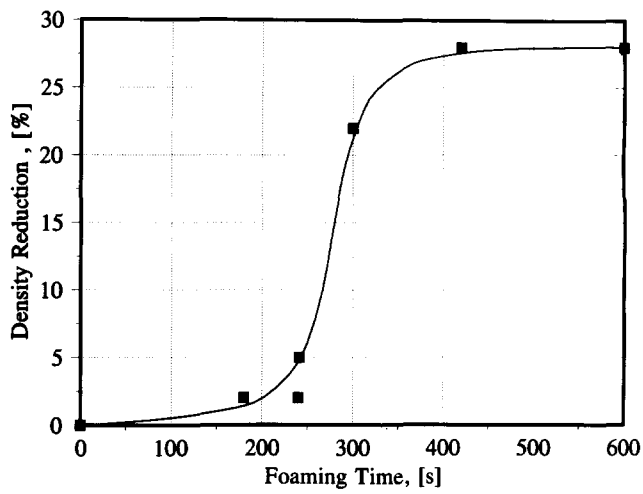

Figure 11 Density reduction as a function of foaming time for samples with n^*-notch geometry foamed at 165°C

shows that the maximum load increases dramatically owing to the foaming process, which means that excessive plastic deformation occurs before the crack starts to grow. Therefore, we believe that the bubbles change the plastic constraint in front of the notch rather than just increasing the effective notch tip radius. Finally, the bubble number density and polymer density reduction (or equivalently, bubble volume fraction) are depicted in *Figures 10* and *11*, respectively. The conditions for the best properties correspond to a bubble number density of about 6 to 7×10^6 bubbles per cm^3, and polymer density reduction of about 28%.

Typical ligament thicknesses in the foamed samples with foaming time above 300 s are between 10 and 15 μm, calculated either by assuming a simple cubic lattice with equal bubble size (bubble diameter of 40 μm and bubble volume fraction of 28%), or from the micrographs. When the root radius is very small (or equivalently, the notch is sharp), the notch creates plane-strain (triaxial-stress) conditions at the tip and the bubbles inside the foam samples are able to transform these conditions into plane-stress conditions. As mentioned in the Introduction, plane-stress conditions correspond to ductile, and thus tough, fracture. Therefore, a brittle-to-tough transition in PC can be achieved by introducing small holes, equivalent to rubber particles.

CONCLUSIONS

PC is brittle under impact conditions in the presence of a sharp notch (n^*-notch geometry). It has been known for a long time that introducing small rubber particles into the PC matrix could induce a transition from brittle to ductile behaviour. The rubber particles act by internal cavitation, thus relieving the triaxial stress state in front of the crack tip. This explanation has led to much speculation as to whether holes might work as impact modifiers. In this work it is proved that bubbles with diameter of about 40 μm, and at a volume fraction of about 28% in PC, are indeed able to increase the notched impact toughness dramatically.

ACKNOWLEDGEMENTS

We gratefully acknowledge the Center for High Performance Polymeric Adhesives and Composites (Grant No. 9120004) and the Center on Innovative Technology (Grant No. MAT-91-004) for support of this work.

REFERENCES

1 Borggreve, R. J. M., Gaymans, R. J. and Eichenwald, H. M. *Polymer* 1989, **30**, 78
2 Van der Sanden, H. C. M., Meijer, H. E. H. and Tervoort, T. A. *Polymer* 1993, **34**, 2148
3 Van der Sanden, H. C. M., Meijer, H. E. H. and Tervoort, T. A. *Polymer* 1993, **34**, 2961
4 Schrenk, W. J. and Alfrey, T. *Polym. Eng. Sci.* 1969, **9**, 393
5 Weymans, G., Berg, K., Morbitzer, L. and Grigo, U. *Angew. Makromol. Chem.* 1988, **162**, 189
6 Rudnev, S. N., Salamatina, O. B., Voenniy, V. V. and Oleynik, E. F. *Colloid Polym. Sci.* 1991, **269**, 460
7 Brown, H. R. *J. Mater. Sci.* 1982, **17**, 469
8 Kinloch, A. J. and Young, R. J. 'Fracture Behavior of Polymers', Applied Science Publishers, London, 1983
9 Sue, H.-J., Huang, J. and Yee, A. F. *Polymer* 1992, **33**, 4868
10 Martini, F., Waldman, F. and Suh, N. P. 42nd SPE Annual Technical Conference, New Orleans, LA, 1984, Vol. 30, p. 674
11 Waldman, F. MS thesis, Mechanical Engineering Department, Massachusetts Institute of Technology, 1982
12 Collias, D. I. and Baird, D. G. *Polym. Eng. Sci.* in press
13 Collias, D. I. and Baird, D. G. *Polym. Eng. Sci.* in press